AN ELASTIC VISCOPLASTIC MODEL FOR THE ANALYSIS OF THE DUCTILE BEHAVIOR OF ROCK SALT

André Luiz Grando Santos, andreluizgarndo@gmail.com
Marcelo Krajnc Alves, Krajnc@emc.ufsc.br
Department of Mechanical Engineering, Federal University of Santa Catarina, Florianópolis, Brazil

Abstract. *This work presents a viscoplastic model for rock salt, proposes an implicit numerical scheme and develops a computer code for the analysis of the ductile behavior of rock salt. The investigated model is based on a multiple creep mechanism approach and incorporates the hardening and recovery behavior of rock salt when subjected to a deformation process. The multiple creep mechanisms are obtained from a deformation map, for natural salt, decribing the steady-state creep response. Here, one considers deepwater oil field development conditions in which the following three mechanisms predominate: dislocation glide, at very high shear stresses; dislocation climb, for high temperatures; and a well characterized but undefined mechanism, for lower shear stresses and temperatures. Constitutive relations for these mechanism are used in order to describe the steady state creep, which are modified in order to describe the transient creep behavior. An implicit numerical scheme is proposed in order to determine approximate numerical solution using the Galerkin Finite Element method. In addition, a continuous consistent tangent operator, associated with the implicit method, is derived by a proper linearization of the weak form of the equilibrium equation. For simplicity, one considers only plane strain and axisymmetric problems and make used of a Tri6 finite element, circumventing the volumetric locking phenomena. With the aim of verifying the adequacy and robustness of the proposed algorithm and implemented code one solves a set of simple problems.*

Keywords: viscoplasticity, rock salt, finite elements

1. INTRODUCTION

The objective of this work is to investigate the rock salt model presented by Munson (1997), propose an implicit numerical scheme for the determination of approximate numerical solutions using the Galerkin Finite Element method and implement a computer code with the aim of analyzing the ductile behavior of rock salt specimens under deepwater oil field development conditions. A consistent tangent operator, associated with the proposed implicit scheme, is also derived. The rock salt model presented by Munson (1997) employs a multi-mechanism deformation map for the modeling of the steady state response of rock salt, under deepwater oil field development conditions. In order to account for work hardening and dynamic recovery that occur under transient creep deformation an internal variable is introduced together with its evolution equation. Also, since the elastic yield stress for rock salt is very small, $\sigma_E < 1\,MPa$, Munson (1997) made use of a viscoplastic model with no yield criterion. Moreover, under deepwater oil field development conditions, which is the focus of this work, experimental observations show that the creeping deformation of rock salt may be approximately as isochoric and that only the first (transient) and second (steady) creep stages must be taken into account, see Fossum and Fredrich (2002) and Fredrich *et al.* (2007). In addition, see Munson and Dawson (1979), Munson and Devries (1991) and Munson (1997), at steady state creep response, the leading creeping mechanisms, for natural salt, are: dislocation glide, at very high shear stresses; dislocation climb, for high temperatures; and a well characterized but undefined mechanism, for lower shear stresses and temperatures. These mechanisms are then employed in the derivation of the steady state creep constitutive equation.

2. THE VISCOPLASTIC ROCK SALT MODEL WITH NO YIELD SURFACE

The model presented by Munson (1997) considers, in order to describe the transient creep stage, a state parameter, *r*, that is related to the work hardening and dynamic recovering behavior of rock salt. Here, for simplicity, the problem is restricted to small displacements and deformations and the deformation process is assumed to be isothermal. The rock salt model proposed by Munson (1997) may be summarized by:

(i) The additive decomposition of the total strain into an elastic part, $\boldsymbol{\varepsilon}^e$, and a viscoplastic part, $\boldsymbol{\varepsilon}^{vp}$, as

$$\boldsymbol{\varepsilon} = \boldsymbol{\varepsilon}^e + \boldsymbol{\varepsilon}^{vp} \tag{1}$$

(ii) The stress versus elastic strain constitutive equation

$$\boldsymbol{\sigma} = \boldsymbol{D}\boldsymbol{\varepsilon}^e \tag{2}$$

in which

$$D_{ijrs} = \mu\left(\delta_{ir}\delta_{js} + \delta_{is}\delta_{jr}\right) + \bar{\lambda}\delta_{ij}\delta_{rs} , \tag{3}$$

where $\mu = \frac{E}{2(1+\nu)}$ (shear modulus) and $\bar{\lambda} = \frac{\nu E}{(1+\nu)(1-2\nu)}$ (Lamé's constant) with E denoting the Young's modulus and ν the Poisson's ratio.

(iii) The viscoplastic flow rule

$$\dot{\varepsilon}^c = \dot{\lambda}N \tag{4}$$

where

$$N = \frac{1}{2}\frac{\sigma^D}{q} + \frac{\eta}{3}I \tag{5}$$

and

$$\dot{\lambda} = \dot{e}_{ef}^{vp} \tag{6}$$

with $\sigma = \sigma^D + pI$, σ^D denoting the deviatoric stress, $p = \frac{1}{3}tr(\sigma)$ the mean (hydrostatic) stress and $q = \sqrt{\frac{1}{2}\left(\sigma^D\right).\left(\sigma^D\right)}$ the effective von Mises stress measure. Here, η is a material parameter that must be identified, $\dot{\lambda}$ denotes the rate of the viscoplastic multiplier and $\dot{e}_{ef}^{vp}$ denotes the rate of the effective strain measure.

(iv) The evolution law for the internal variable, r, is given by

$$\dot{r} = \left\{\frac{\left(F(\sigma,r)-1\right)}{F(\sigma,r)}\right\}\dot{\lambda} = \left(F(\sigma,r)-1\right)\dot{e}_{ef(s)}^{vp} \tag{7}$$

in which

$$F(\sigma,r) = \begin{cases} \exp\left\{\delta_1(\sigma)\left(1-\left(\frac{r}{\varepsilon_t^*(\sigma)}\right)\right)^2\right\}; & r < \varepsilon_t^*(\sigma) \\ 1 \\ \exp\left\{\delta_2(\sigma)\left(1-\left(\frac{r}{\varepsilon_t^*(\sigma)}\right)\right)^2\right\}; & r > \varepsilon_t^*(\sigma) \end{cases} \tag{8}$$

where

$$\delta_1(\sigma) = \alpha_w + \beta_w \log\left(\frac{q}{\mu}\right) \tag{9}$$

$$\delta_2(\sigma) = \alpha_r + \beta_r \log\left(\frac{q}{\mu}\right) \tag{10}$$

$$\varepsilon_t^*(\sigma) = K_o^*\left(\frac{q}{\mu}\right)^m , \quad K_o^* = K_o \exp\{c_o T\} \tag{11}$$

and

$$\dot{e}^{vp}_{ef(s)} = \dot{e}^{vp}_{ef(1)} + \dot{e}^{vp}_{ef(2)} + \dot{e}^{vp}_{ef(3)} \tag{12}$$

where

$$\dot{e}^{vp}_{ef(s_1)} = A_1^* \left(\frac{q}{\mu}\right)^{n_1}, \quad A_1^* = A_1 \exp\left\{\frac{-Q_1}{RT}\right\} \tag{13}$$

$$\dot{e}^{vp}_{ef(s_2)} = A_2^* \left(\frac{q}{\mu}\right)^{n_2}, \quad A_2^* = A_2 \exp\left\{\frac{-Q_2}{RT}\right\} \tag{14}$$

and

$$\dot{e}^{vp}_{ef(s_3)} = H\left(q - \sigma_o\right) B_o \sinh\left[\frac{\overline{q}(q - \sigma_o)}{\mu}\right], \quad B_o = \left[B_1 \exp\left\{\frac{-Q_1}{RT}\right\} + B_2 \exp\left\{\frac{-Q_2}{RT}\right\}\right]. \tag{15}$$

Here, A_1, A_2, Q_1, Q_2 B_1, B_2, R, σ_o, $\overline{q}$, c_o, K_o, m, n_1, n_2, α_w, β_w, α_r, β_r are material parameters and T is the absolute temperature at which the specimen is subjected.

3. DISCRETIZATION OF THE ROCK SALT MODEL

In order to derive the fully implicit algorithm, one assume the solution to be known in the interval $\left[0, t_n\right]$ and imposes the equilibrium condition at t_{n+1}. As a result, one derives the following weak form: Determine $\vec{u}_{n+1} \in \mathbf{K}$ so that

$$\int_\Omega \boldsymbol{\sigma}_{n+1} \boldsymbol{\varepsilon}(\vec{w}) \, d\Omega = \int_{\Gamma_t} \vec{t}_{n+1}.\vec{w} \, d\Gamma + \int_\Omega \rho \vec{b}_{n+1}.\vec{w} \, d\Omega, \forall \vec{w} \in \mathbf{V}_u. \tag{16}$$

in which $\mathbf{K}$ represents the set of admissible displacements and $\mathbf{V}_u$ the set of admissible variations.

3.1. Operator Split Algorithm

Here, in order to improve the robustness of the algorithm, one applies the operator split strategy, see Souza Neto *et al.* (2008), described by:

(i) The trial elastic step problem, formulated as: Given the strain history $\{\varepsilon(t)\} \in [t_n, t_{n+1}]$, find $\varepsilon^{e\,trial}_{n+1}$ and r^{trial}_{n+1} so that $\dot{\varepsilon}^{e\,trial} = \dot{\varepsilon}$ and $\dot{r}^{trial} = 0$. As a result, one derives

$$\varepsilon^{e\,trial}_{n+1} = \varepsilon_{n+1} - \varepsilon^{vp}_n \quad \text{and} \quad r^{trial}_{n+1} = r_n. \tag{17}$$

Once $\varepsilon^{e\,trial}_{n+1}$ is determined, one computes $e^{e\,trial}_{H_{n+1}} = \frac{1}{3} tr\left[\boldsymbol{\varepsilon}^{e\,trial}_{n+1}\right]$, $\boldsymbol{\varepsilon}^{e\,D\,trial}_{n+1} = \boldsymbol{\varepsilon}^{e\,trial}_{n+1} - e^{e\,trial}_{H_{n+1}}\mathbf{I}$ and the trial elastic stresses $p^{trial}_{n+1} = \frac{E}{(1-2\nu)} e^{e\,trial}_{H_{n+1}}$ and $\sigma^{D\,trial}_{n+1} = 2G\varepsilon^{e\,D\,trial}_{n+1}$.

(ii) The viscoplastic return mapping step problem
Here, by applying the fully implicit Euler method and performing some additional algebra, one derives the following coupled nonlinear problem, stated as: Given ε_{n+1}, determine $\left(r_{n+1}, p_{n+1}, q_{n+1}\right)$ that satisfies:

$$R_1\left(r_{n+1}, p_{n+1}, q_{n+1}\right) = r_{n+1} - r_n - \left(F\left(r_{n+1}, q_{n+1}\right) - 1\right) \Delta e^{vp}_{ef(s)}\left(q_{n+1}\right) = 0 \tag{18}$$

$$R_2\left(r_{n+1}, p_{n+1}, q_{n+1}\right) = p_{n+1} + \frac{\eta E}{3(1-2\nu)} F\left(r_{n+1}, q_{n+1}\right) \Delta e^{vp}_{ef(s)}\left(q_{n+1}\right) - p^{trial}_{n+1} = 0 \tag{19}$$

$$R_3\left(r_{n+1}, p_{n+1}, q_{n+1}\right) = q_{n+1} + \mu F\left(r_{n+1}, q_{n+1}\right) \Delta e^{vp}_{ef(s)}\left(q_{n+1}\right) - q^{trial}_{n+1} = 0 \tag{20}$$

where

$$\Delta\, e_{ef(s)}^{vp}\left(q_{n+1}\right) = \Delta\, e_{ef(1)}^{vp}\left(q_{n+1}\right) + \Delta\, e_{ef(2)}^{vp}\left(q_{n+1}\right) + \Delta\, e_{ef(3)}^{vp}\left(q_{n+1}\right) \tag{21}$$

with

$$\Delta\, e_{ef(1)}^{vp}\left(q_{n+1}\right) = A_1^*\left(\frac{q_{n+1}}{\mu}\right)^{n_1}\Delta\, t \tag{22}$$

$$\Delta\, e_{ef(2)}^{vp}\left(q_{n+1}\right) = A_2^*\left(\frac{q_{n+1}}{\mu}\right)^{n_2}\Delta\, t \tag{23}$$

and

$$\Delta\, e_{ef(3)}^{vp}\left(q_{n+1}\right) = H\left(q_{n+1} - \sigma_o\right)B_o\sinh\left[\frac{\bar{q}\left(q_{n+1}-\sigma_o\right)}{\mu}\right]\Delta\, t \tag{24}$$

in which $\Delta\, t = t_{n+1} - t_n$.

Now, once $\left(r_{n+1}, p_{n+1}, q_{n+1}\right)$ is computed it is possible to compute the Cauchy stress as follows:

$$\Delta\,\lambda = F\left(r_{n+1}, q_{n+1}\right)\Delta\, e_{ef(s)}^{vp}\left(q_{n+1}\right) \tag{25}$$

$$\boldsymbol{\sigma}_{n+1}^{D} = \boldsymbol{\sigma}_{n+1}^{D\,trial}\left[1 + \frac{\mu\,\Delta\,\lambda}{q_{n+1}}\right]^{-1} \tag{26}$$

so that

$$\boldsymbol{\sigma}_{n+1} = \boldsymbol{\sigma}_{n+1}^{D} + p_{n+1}\mathbf{I}. \tag{27}$$

Moreover, one may compute the viscoplastic strain, $\boldsymbol{\varepsilon}_{n+1}^{vp}$, and the effective viscoplastic strain, $e_{ef_{n+1}}^{vp}$, as

$$\boldsymbol{\varepsilon}_{n+1}^{vp} = \boldsymbol{\varepsilon}_n^{vp} + \Delta\,\lambda\left[\frac{1}{2}\frac{\boldsymbol{\sigma}_{n+1}^{D}}{q_{n+1}} + \frac{\eta}{3}\mathbf{I}\right] \tag{28}$$

and

$$e_{ef_{n+1}}^{vp} = e_{ef_n}^{vp} + \Delta\,\lambda. \tag{29}$$

3.2. Incremental weak formulation of the problem

Once defined the constitutive model, one may solve the global equilibrium problem by employing an incremental procedure. The incremental formulation between t_n and t_{n+1} considers that

$$\vec{u}_{n+1} = \vec{u}_n + \Delta\,\vec{u}_n \tag{30}$$

so that, at time t_{n+1}, the weak formulation of the problem may be stated as: Determine $\vec{u}_{n+1}\in\mathbf{K}$, which solves

$$F_1\left(\vec{u}_{n+1};\vec{w}\right) = \int_\Omega\boldsymbol{\sigma}_{n+1}.\boldsymbol{\varepsilon}\left(\vec{w}\right)\,d\Omega - \int_\Omega\rho\,\vec{b}_{n+1}.\vec{w}\,d\Omega - \int_{\Gamma^t}\vec{t}_{n+1}.\vec{w}\,dA = 0,\quad\forall\vec{w}\in\mathbf{V}_{\boldsymbol{u}} \tag{31}$$

Since the above problem is non-linear, one applies Newton's method leading to the solution of a sequence of linearized problems.

Linearization procedure

Let $\vec{u}_{n+1}^{k}$ be the estimate solution of (25) at the *k-th* iteration and consider that

$$\vec{u}_{n+1}^{k} = \vec{u}_n\ \text{at}\ k = 0. \tag{32}$$

For the *k-th* iteration of the solution procedure, one has

$$\vec{u}_{n+1}^{k+1} = \vec{u}_{n+1}^{k} + \Delta\vec{u}_{n+1}^{k}. \tag{33}$$

The determination of the increment $\Delta \vec{u}_{n+1}^k$ is obtained by imposing

$$F_1\left(\vec{u}_{n+1}^k + \Delta \vec{u}_{n+1}^k; \vec{w}\right) = 0, \quad \forall \vec{w} \in \mathbf{V}_u. \tag{34}$$

Considering $F_1(\circ)$ being Gateaux differentiable one derive the first order approximation given by

$$F_1\left(\vec{u}_{n+1}^k + \boldsymbol{\Delta} \vec{u}_{n+1}^k; \vec{w}\right) \simeq F_1\left(\vec{u}_{n+1}^k; \vec{w}\right) + DF_1\left(\vec{u}_{n+1}^k; \vec{w}\right)\left[\boldsymbol{\Delta} \vec{u}_{n+1}^k\right]. \tag{35}$$

Now, replacing (35) into (34) finally yields

$$DF_1\left(\vec{u}_{n+1}^k; \vec{w}\right)\left[\Delta \vec{u}_{n+1}^k\right] = -F_1\left(\vec{u}_{n+1}^k; \vec{w}\right) \tag{36}$$

where

$$DF_1\left(\vec{u}_{n+1}^k; \vec{w}\right)\left[\Delta \vec{u}_{n+1}^k\right] = \lim_{\varepsilon \to 0} \frac{F_1\left(\vec{u}_{n+1}^k + \varepsilon \Delta \vec{u}_{n+1}^k; \vec{w}\right) - F_1\left(\vec{u}_{n+1}^k; \vec{w}\right)}{\varepsilon} = \frac{d}{d\varepsilon}\left[F_1\left(\vec{u}_{n+1}^k + \varepsilon \Delta \vec{u}_{n+1}^k; \vec{w}\right)\right]_{\varepsilon=0}. \tag{37}$$

Since Ω is fixed and the prescribed traction and body forces are assumed to be independent of the displacement field, one derives

$$DF_1\left(\vec{u}_{n+1}^k; \vec{w}\right)\left[\Delta \vec{u}_{n+1}^k\right] = \int_\Omega \frac{d}{d\varepsilon}\left[\sigma_{n+1}\left(\varepsilon\left(\vec{u}_{n+1}^k\right)\right)\right]_{\varepsilon=0} \cdot \varepsilon(\vec{w}) \ d\Omega = \int_\Omega \left[D_T\left(\vec{u}_{n+1}^k\right)\right]_{ijkl} \varepsilon_{kl}\left(\Delta \vec{u}_{n+1}^k\right) \cdot \varepsilon_{ij}(\vec{w}) \ d\Omega \tag{38}$$

in which $\left[D_T\left(\vec{u}_{n+1}^k\right)\right]_{ijkl} = \dfrac{\partial \sigma_{ij}}{\partial \varepsilon_{kl}}\left(\vec{u}_{n+1}^k\right)$ is the consistent tangent modulus.

3.3. Determination of the consistent tangent modulus

The consistent tangent operator is given by

$$\left[\mathbf{D_T}\right]_{ijkl} = \frac{\partial \boldsymbol{\sigma}_{ij}}{\partial \boldsymbol{\varepsilon}_{kl}} = \frac{\partial \boldsymbol{\sigma}_{ij}}{\partial \boldsymbol{\varepsilon}_{kl}^{trial}} \tag{39}$$

Now, since $\sigma_{ij} = \sigma_{ij}^D + p\delta_{ij}$, one derives

$$[D_T]_{ijkl} = \frac{\partial \sigma_{ij}^D}{\partial \varepsilon_{kl}^{trial}} + \frac{\partial p}{\partial \varepsilon_{kl}^{trial}} \delta_{ij} \tag{40}$$

However, $\sigma_{ij}^D = \left[\dfrac{q_{n+1}}{q_{n+1} + \mu \, \Delta \lambda}\right]\sigma_{ij}^{D^{trial}}$, which yields

$$\frac{\partial \sigma_{ij}^D}{\partial \varepsilon_{kl}^{trial}} = \left[\frac{q_{n+1}}{q_{n+1} + \mu \, \Delta \lambda}\right]\left\{\frac{\partial \sigma_{ij}^{D^{trial}}}{\partial \varepsilon_{kl}^{trial}} + \frac{\sigma_{ij}^{D^{trial}}}{q_{n+1}}\frac{\partial q_{n+1}}{\partial \varepsilon_{kl}^{trial}} - \frac{\sigma_{ij}^{D^{trial}}}{\left[q_{n+1} + \mu \, \Delta \lambda\right]}\left(\frac{\partial q_{n+1}}{\partial \varepsilon_{kl}^{trial}} + \mu \frac{\partial \Delta \lambda}{\partial \varepsilon_{kl}^{trial}}\right)\right\} \tag{41}$$

also, $\Delta \lambda = F\left(r_{n+1}, q_{n+1}\right) \Delta \, e_{ef(s)}^{vp}\left(q_{n+1}\right)$, which gives

$$\frac{\partial \Delta \lambda}{\partial \varepsilon_{kl}^{trial}} = \frac{\partial \Delta \lambda}{\partial r_{n+1}} \frac{\partial r_{n+1}}{\partial \varepsilon_{kl}^{trial}} + \frac{\partial \Delta \lambda}{\partial q_{n+1}} \frac{\partial q_{n+1}}{\partial \varepsilon_{kl}^{trial}} \tag{42}$$

in which

$$\frac{\partial \Delta \lambda}{\partial r_{n+1}} = \Delta\, e^{vp}_{ef(s)}\, \frac{\partial F}{\partial r_{n+1}} \tag{43}$$

and

$$\frac{\partial \Delta \lambda}{\partial q_{n+1}} = \frac{\partial F}{\partial q_{n+1}}\, \Delta\, e^{vp}_{ef(s)} + F\, \frac{\partial \Delta e^{vp}_{ef(s)}}{\partial q_{n+1}}. \tag{44}$$

Now, from the trial elastic step solution one derives

$$\frac{\partial p^{trial}}{\partial \varepsilon^{e\,trial}_{kl}} = \frac{E}{3(1-2\nu)}\delta_{kl} \tag{45}$$

$$\frac{\partial \sigma^{D\,trial}_{ij}}{\partial \varepsilon^{e\,trial}_{kl}} = 2\mu\left\{\delta_{ik}\delta_{jl} - \tfrac{1}{3}\delta_{kl}\delta_{ij}\right\} \tag{46}$$

and

$$\frac{\partial q^{trial}}{\partial \varepsilon^{e\,trial}_{kl}} = \mu\, \frac{\sigma^{D\,trial}_{kl}}{q^{trial}} \tag{47}$$

Finally, in order to compute $\frac{\partial p_{n+1}}{\partial \varepsilon_{ij}} = \frac{\partial p_{n+1}}{\partial \varepsilon^{e\,trial}_{ij}}$, $\frac{\partial q_{n+1}}{\partial \varepsilon_{ij}} = \frac{\partial q_{n+1}}{\partial \varepsilon^{e\,trial}_{ij}}$ and $\frac{\partial r_{n+1}}{\partial \varepsilon_{ij}} = \frac{\partial r_{n+1}}{\partial \varepsilon^{e\,trial}_{ij}}$ one notice that the solution of (18-20), given

by $(r_{n+1}, p_{n+1}, q_{n+1})$, is obtained for a given value of $\boldsymbol{\varepsilon}_{n+1}$. However, $\boldsymbol{\varepsilon}^{e\,trial}_{n+1} = \boldsymbol{\varepsilon}_{n+1} - \boldsymbol{\varepsilon}^{vp}_n$ and $\boldsymbol{\varepsilon}^{vp}_n$ is a constant, at t_{n+1}, which allow us to conclude that

$$q_{n+1} = q_{n+1}\left(\boldsymbol{\varepsilon}^{e\,trial}_{n+1}\right) \tag{48}$$

$$p_{n+1} = p_{n+1}\left(\boldsymbol{\varepsilon}^{e\,trial}_{n+1}\right) \tag{49}$$

and

$$r_{n+1} = r_{n+1}\left(\boldsymbol{\varepsilon}^{e\,trial}_{n+1}\right). \tag{50}$$

As a result, differentiating (48-50) with respect to $\boldsymbol{\varepsilon}^{e\,trial}_{n+1}$ leads to a linear system of equations that may be solved for $\frac{\partial p_{n+1}}{\partial \varepsilon_{ij}}$, $\frac{\partial q_{n+1}}{\partial \varepsilon_{ij}}$ and $\frac{\partial r_{n+1}}{\partial \varepsilon_{ij}}$.

4. NUMERICAL EXAMPLES

The discretization of the problem is obtained by the application of the Galerkin Finite Element method using a Tri 6 element. In order to verify the adequacy of the model and the proposed implicit algorithm, one solves a set of simple problems. The parameters used in these examples are given in "Table 1".

Table 1. Parameters employed by the model

$E = 31\ GPa$	$\nu = 0.25$	$A_1^* = 9.8891 \times 10^{11}\ s^{-1}$
$n_1 = 5.5$	$A_2^* = 4.11299 \times 10^{08}\ s^{-1}$	$n_2 = 5.0$
$\bar{q} = 5.335 \times 10^{03}$	$\boldsymbol{\sigma}_o = 20.57 MPa$	$B_o = 1.29 \times 10^{06}\ s^{-1}$
$\alpha_w = -17.37$	$\beta_w = -7.738$	$\alpha_r = 0.58$
$\beta_r = 0.0$	$m = 3$	$K_o^* = 6.2364 \times 10^{07}$
$\eta = 0.1$	$\mu = 12.4\ GPa$	

4.1. Axial compression

Here, one considers a cylindrical rock salt specimen subjected to an axial loading, applied by prescribing an axial displacement. The specimen has a length of *100mm* and a diameter of *50 mm*. The compression loading resulted from a prescribed displacement, applied by a linear ramp, ranging from zero to a maximum value of $\bar{u} = 10mm$. The uniaxial compression tests were performed at four different strain rates, given respectively by $3.33 \times 10^{-4} s^{-1}$, $5.55 \times 10^{-5} s^{-1}$, $2.77 \times 10^{-5} s^{-1}$ and $1.37 \times 10^{-6} s^{-1}$, as depicted in Figure 1.
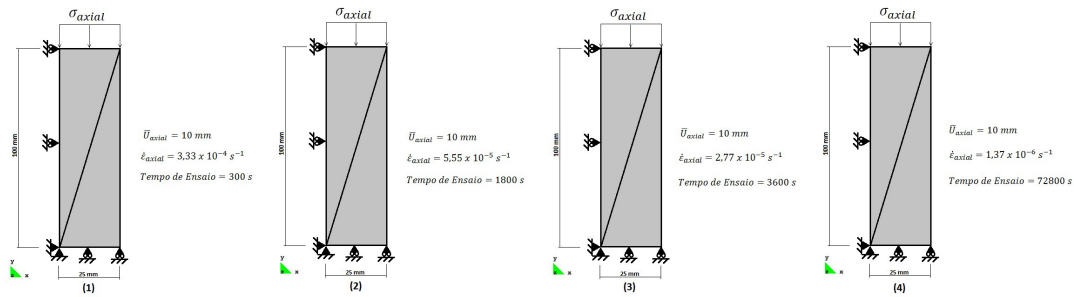
Fig. 1 – Description of the uniaxial compression tests

Figure 1 also contains the time duration of each uniaxial compression test. These analysis employed 1000 incremental displacement steps and used a convergence tolerance of 1.0×10^{-6}.

The stress-strain curves relating the absolute values of the axial stress σ_{yy} with the absolute value of the axial strain ε_{yy}, obtained for each test, are depicted in Figure 2.
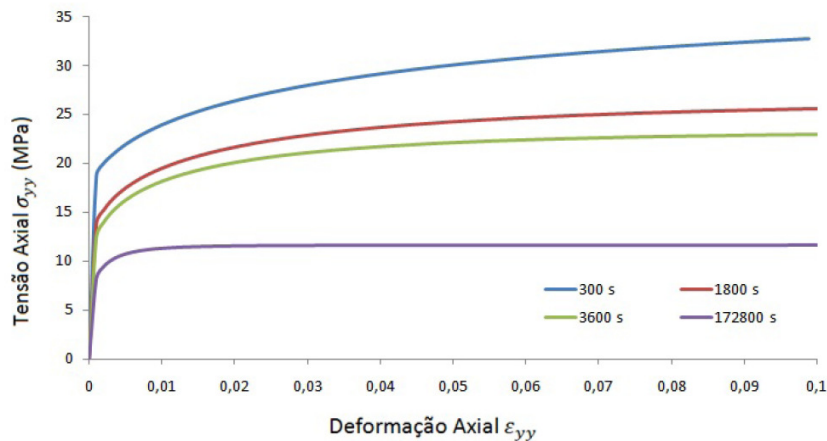
Fig. 2 – Stress-Strain results for the uniaxial compression tests

4.2. Triaxial compression

Here, one considers a cylindrical rock salt specimen subjected to a lateral confining pressure together with an axial "compression loading", resulting from the application of a prescribed displacement history. The specimen has a length of *100mm* and a diameter of *50 mm*. The prescribed displacement resulted from the application of a linear ramp, ranging from zero to a maximum value of $\bar{u} = 10mm$. The tests were performed with a strain rate of $3.33 \times 10^{-4} s^{-1}$, for a loading time of 300 seconds and by considering the following lateral confining stresses: *5MPa*, *10MPa* and *15MPa* respectively, as depicted in Figure 3. A total of 1000 displacement increments were applied and employed a convergence tolerance of 1.0×10^{-6}.
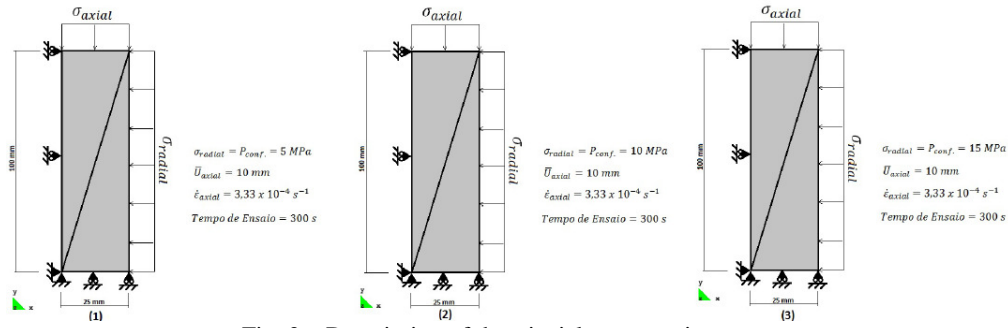
Fig. 3 – Description of the triaxial compression test.

The stress-strain curves relating the absolute values of the axial stress $\boldsymbol{\sigma}_{yy}$ with the absolute value of the axial strain $\boldsymbol{\varepsilon}_{yy}$, obtained for each test, are depicted in Figure 4.
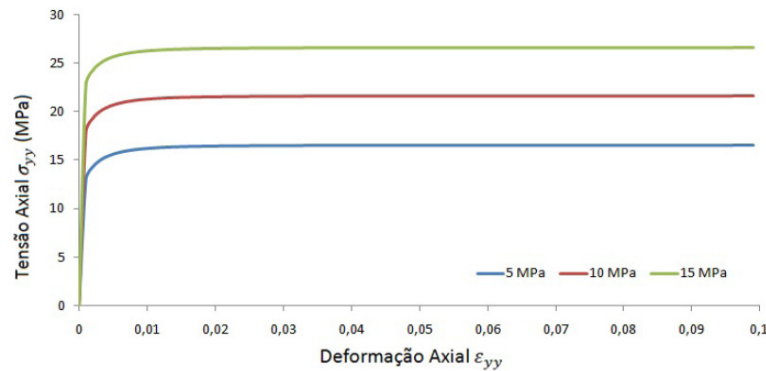

Fig. 4 – Stress-strain curves (absolute value) for different confining pressures.

4.3. Uniaxial creeping test

Here, one considers a cylindrical rock salt specimen subjected to a step load consisting of a constant compressive stress. The specimen has a length of *100mm* and a diameter of *50 mm*. The test was performed for three different loading conditions, given by a load step of *5MPa*, *10MPa* and *15MPa* respectively, which were applied for 86400 seconds, as depicted in Figure 5.
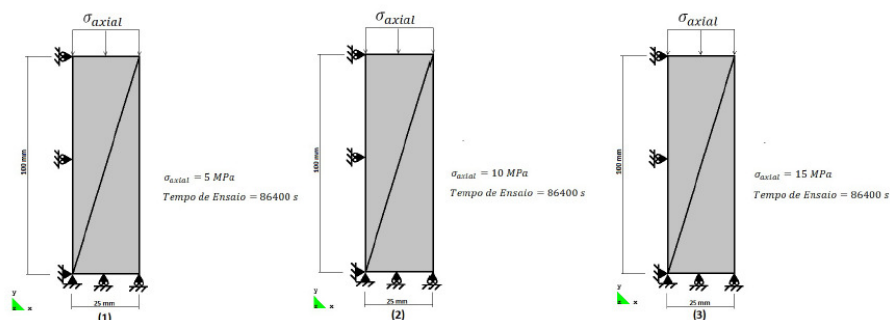

Fig. 5 – Description of the creeping compression test.

The time evolutions of the absolute value of the axial viscoplastic strain, for each of the different constant load steps, are depicted in Figure 6.
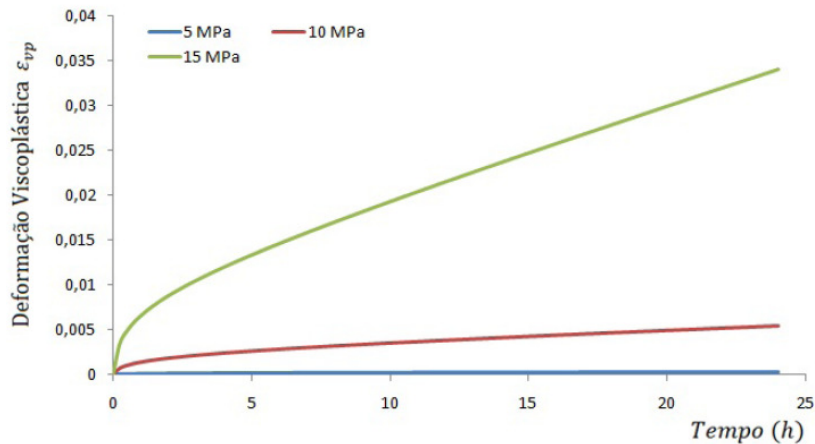
Fig. 6 – Evolution of the axial viscoplastic strain in a creep test

4.4. Diametrical compression test

Here, one considers a diametrical compression test of a rock salt specimen, as depicted in Figure 7. The problem is considered to be subjected to a plane strain condition and due to symmetry conditions only one fourth of the domain was modeled. The specimen is subjected to a prescribed displacement applied by a linear ramp rangimg from zero to a maximum displacement of $\bar{u} = -0.152mm$ corresponding to a constant strain rate of $2.0 \times 10^{-6} s^{-1}$.
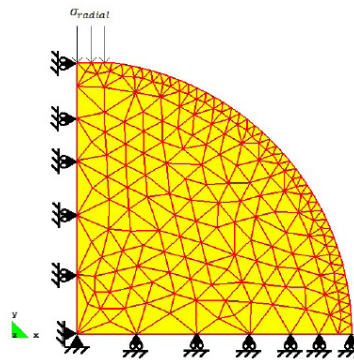

Fig. 7 – Description of the diametrical compression test

Figure 8 shows the distribution of the level sets representing the displacement components, u_x and u_y respectively, at the end of the analysis.
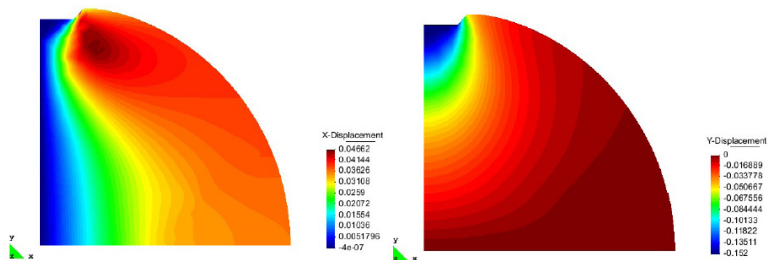

Fig. 8 – Distribution of the level sets of the displacement components u_x and u_y

Figure 9 shows the distribution of the level sets representing the viscoplastic strains $\boldsymbol{\varepsilon}_{xx}^{vp}$ and $\boldsymbol{\varepsilon}_{yy}^{vp}$ at the end of the analysis.
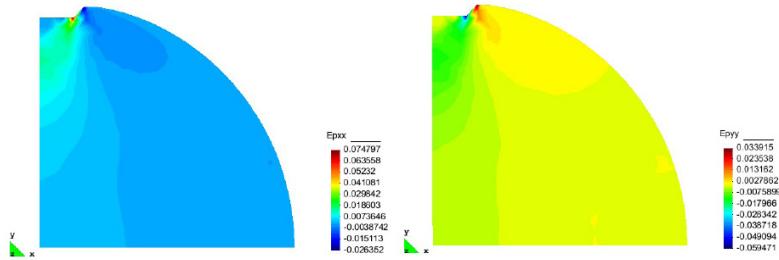
Fig. 9 – Distribution of the level sets of the viscoplastic strain components $\boldsymbol{\varepsilon}_{xx}^{vp}$ and $\boldsymbol{\varepsilon}_{yy}^{vp}$

Figure 10 shows the distribution of the level sets representing the stress component, $\boldsymbol{\sigma}_{xx}$ and $\boldsymbol{\sigma}_{yy}$, at the end of the analysis.
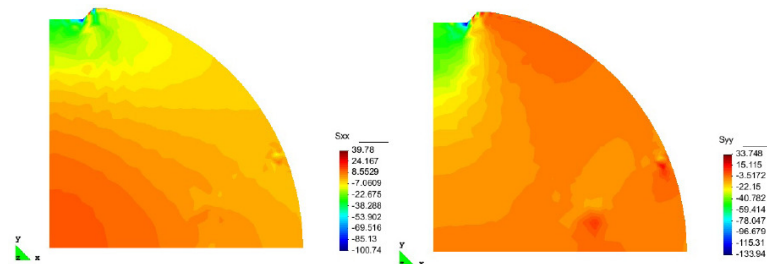
Fig. 10 - Distribution of the level sets of the stress components $\boldsymbol{\sigma}_{xx}$ and $\boldsymbol{\sigma}_{yy}$

5. CONCLUSIONS

The proposed implicit numerical scheme made use of the fully implicit Euler method in the discretization of the evolution equations and have shown to be robust in solving the proposed examples. A continuous consistent tangent operator was derived, associated with the proposed implicit scheme assuring the quadratic convergence rate of Newton's method. In order to improve the solution for the stress components, see Figure 10, it is necessary to consider a more refined mesh. The problem illustrated in Figure 7 is a simplified model of an experimental diametrical compression test. The proper modeling of such tests requires the usage of unilateral contact conditions at the loading surface, which was not implemented. Due to the simplified modeling one can see a large plastic flow of the rock salt in the neighborhood of the loading surface.

6. ACKNOWLEDGEMENTS

7. REFERENCES

Souza Neto, E.A., Peric D., Owens D., 2008. "Computational methods for plasticity: theory and applications", John Wiley & Sons Ltd.

Fossum A. F. and Fredrich J. T, 2002, "Salt Mechanics Primer for Near-Salt and Sub-Salt Deepwater Gulf of Mexico Field Developments", Report Sandia National Laboratories.

Fredrich, J.T., Fossum, A.F. and Hickman, R.J., 2007, "Mineralogy of deepwater Gulf of Mexico salt formations and implications for constitutive behavior", Journal of Petroleum Science and Engineering Vol. 57,pp. 354-374.

Munson, D.E., 1997. "Constitutive Model of Creep in Rock Salt Applied to Underground Room Closure", Int. J. Rock Mech. Min. Sci., vol. 34, no 2, pp. 233-247.

Munson, D. E.; Dawson, P. R., 1979, "Constitutive Model for the Low Temperature Creep of Salt", SAND79-1853, Sandia National Laboratories, 1979.

Munson, D. E.; Devries, K. L., 1991, "Development and Validation of a Predictive Technology for Creep Closure of Underground Rooms in Salt", Seventh International Congress on Rock Mechanics, vol 1, pp 127-134, Aachen/Deutschland.

8. RESPONSIBILITY NOTICE

The authors are the only responsible for the printed material included in this paper.